

Structure of the β 2- α 2 loop and interspecies prion transmission

Cyrus Bett,^{*,†,1} Natalia Fernández-Borges,^{‡,1} Timothy D. Kurt,^{*,†} Melanie Lucero,^{*,†} K. Peter R. Nilsson,[§] Joaquín Castilla,^{‡,||} and Christina J. Sigurdson^{*,†,1,2}

^{*}Department of Pathology and [†]Department of Medicine, University of California, San Diego, La Jolla, California, USA; [‡]Center for Cooperative Research in Biosciences (CIC bioGUNE), Parque Tecnológico de Bizkaia, Derio, Spain; [§]Department of Physics, Chemistry, and Biology, Linköping University, Linköping, Sweden; ^{||}Basque Foundation for Science (IkerBasque), Bilbao, Spain; and ¹Department of Pathology, Microbiology, and Immunology, University of California, Davis, California, USA

ABSTRACT Prions are misfolded, aggregated conformers of the prion protein that can be transmitted between species. The precise determinants of interspecies transmission remain unclear, although structural similarity between the infectious prion and host prion protein is required for efficient conversion to the misfolded conformer. The β 2- α 2 loop region of endogenous prion protein, PrP^C, has been implicated in barriers to prion transmission. We recently discovered that conversion was efficient when incoming and host prion proteins had similar β 2- α 2 loop structures; however, the roles of primary *vs.* secondary structural homology could not be distinguished. Here we uncouple the effect of primary and secondary structural homology of the β 2- α 2 loop on prion conversion. We inoculated prions from animals having a disordered or an ordered β 2- α 2 loop into mice having a disordered or an ordered loop due to a single residue substitution (D167S). We found that prion conversion was driven by a homologous primary structure and occurred independently of a homologous secondary structure. Similarly, cell-free conversion using PrP^C from mice with disordered or ordered loops and prions from 5 species correlated with primary but not secondary structural homology of the loop. Thus, our findings support a model in which efficient interspecies prion conversion is determined by small stretches of the primary sequence rather than the secondary structure of PrP.—Bett, C., Fernández-Borges, N., Kurt, T. D., Lucero, M., Nilsson, K. P. R., Castilla, J., Sigurdson, C. J. Structure of the β 2- α 2 loop and interspecies prion transmission. *FASEB J.* 26, 2868–2876 (2012). www.fasebj.org

Abbreviations: BSE, bovine spongiform encephalopathy; CWD, chronic wasting disease; GdnHCl, guanidine hydrochloride; HRP, horseradish peroxidase; NaPTA, sodium phosphotungstic acid; PMCA, protein misfolding cyclic amplification; PK, proteinase K; PrP, prion protein; PrP^C, cellular prion protein; PrP^{Sc}, scrapie-associated prion protein; PTAA, polythiophene acetic acid; RL, rigid loop; RML, Rocky Mountain Laboratory; saPMCA, serial automated protein misfolding cyclic amplification; WT, wild-type

Key Words: amyloid • TSE • transmissible spongiform encephalopathy • neurodegeneration

PRIONS HAVE BEEN RESPONSIBLE for widespread epidemics, such as the bovine spongiform encephalopathy (BSE) epidemic (1), and are the only known infectious agents that consist of an aggregated protein (2). Prions are transmitted when an aggregated, β -sheet-rich isoform of the prion protein (PrP^{Sc}, scrapie-associated prion protein) templates the misfolding and aggregation of the endogenous cellular prion protein (PrP^C) in a self-propagating process (3). Once in the central nervous system, prion aggregates spread throughout the brain and spinal cord, inciting progressive and ultimately fatal neurodegeneration.

Although intraspecies prion transmission is most common, interspecies transmission also occurs. For example, BSE infects not only cattle but also humans, cats, and zoo animals (4–9). However, predicting when and how prions infect another species is not currently possible. Prion transmission studies have shown that at least two factors are essential to interspecies conversion: PrP^{Sc}:PrP^C sequence identity, with certain residue positions having a strong influence, and the PrP^{Sc} conformation (10). The critical residue positions may vary, depending on the incoming PrP^{Sc} conformation. Even a single residue difference between PrP^C and PrP^{Sc} can alter the PrP^{Sc} conformation or prevent prion propagation (11, 12).

Mature PrP^C consists of ~209 aa and contains a flexibly unstructured N-terminal region and a globular C-terminal domain consisting of 3 α -helices and a short antiparallel β -sheet (13, 14). Although PrP^C is highly conserved among mammals, the β 2- α 2 loop at residues 165–175 (human numbering; ref. 15) is a site of structural diversity and has been hypothesized as a site

¹ These authors contributed equally to this work.

² Correspondence: Department of Pathology, University of California, San Diego, CA, USA. E-mail: csigurdson@ucsd.edu
doi: 10.1096/fj.11-200923

This article includes supplemental data. Please visit <http://www.fasebj.org> to obtain this information.

that influences species barriers (16). The secondary structure of the $\beta 2$ - $\alpha 2$ loop is polymorphic, in that loop sequences containing the 170S are generally poorly defined, whereas sequences containing the 170N or 170N and 174T are well-defined or "rigid" in the NMR solution structures at 20°C (17, 18). In addition, a $\beta 2$ - $\alpha 2$ loop peptide has been shown to form a steric zipper structure: a pair of tightly packed, highly complementary β -sheets proposed to comprise the spine of the amyloid fibril (19, 20).

Single residues within the $\beta 2$ - $\alpha 2$ loop strongly affect prion transmission in nature and in experimental studies. For example, sheep have a naturally occurring polymorphism at residue 172 (Q/R, human numbering), where PrP^C containing 172R is highly protective against classic strains of sheep scrapie. Experimentally, residue 172 also has a major influence on prion conversion in that basic residues at this position can prevent PrP^{Sc} formation *in vitro* (21). Interestingly, identity at loop residue 170 correlated with efficient PrP^C conversion when brain samples from 15 species were seeded with prions from deer with chronic wasting disease (CWD; refs. 22, 23).

To study how the loop structure influences species barriers, we previously inoculated prions from 5 species into 2 lines of transgenic mice expressing either disordered or ordered loop structures due to sequence variations at positions 170 and 174 (24). The loop sequence had a profound effect on species barriers. The rigid loop (RL) mice (170N, 174T) showed inefficient or no PrP conversion in the presence of cattle, sheep, and mouse-adapted prions, which express a heterologous serine residue at position 170. In contrast, RL mouse PrP converted deer and hamster prions, which express a homologous asparagine at position 170. Prion susceptibility was switched in mice expressing the disordered loop variant (170S). Mice were highly susceptible to cattle, sheep, and mouse prions (170S) and weakly susceptible to deer and hamster prions (170N). Because both the primary and secondary structure of PrP^C had been modified, it was unclear whether the switch in transmission barriers observed in the RL mice was due to the new primary or secondary RL structure.

Here we sought to refine our understanding of the role of primary *vs.* secondary structure on cross-species prion transmission. To that end, we used transgenic mice that express mouse PrP with an ordered RL, but due to a single residue substitution, D167S (MoPrP^{167S}; ref. 25). We intracerebrally inoculated prions from species having a disordered or an ordered RL into mice expressing MoPrP or MoPrP^{167S} and performed further seeding studies *in vitro*. We found that MoPrP^{167S} showed no detectable conversion from prions of species having similar ordered RLs yet were highly susceptible to prions from species having disordered loops. Thus, the homologous RL secondary structure had no effect on species barriers. Instead, primary loop sequence homology better predicted efficient conversion. Together with studies of our previously generated RL mice, these findings indicate that the primary sequence of PrP^C and PrP^{Sc} at the $\beta 2$ - $\alpha 2$ loop drives transmission barriers for certain strains *in vivo*.

MATERIALS AND METHODS

Prion inoculations

Wild-type (WT; C57BL/6) or *Tg*(MoPrP^{167S}) mice (groups of $n=4-6$; ref. 26) were intracerebrally inoculated into the left parietal cortex with 30 μ l of brain homogenate containing Rocky Mountain Laboratory (RML) mouse scrapie prions or CWD prions from a naturally infected mule deer previously shown to contain infectious prions (27). Uninfected brain homogenate was inoculated into the same mouse genotypes as a negative control. Mice were monitored 3 times weekly, and transmissible spongiform encephalopathy was diagnosed according to clinical criteria including ataxia, kyphosis, stiff tail, hind leg clasp, and hind leg paresis. Mice were sacrificed at the onset of terminal disease when they showed signs including weight loss, tremors, slow movements, and severe kyphosis or by ~ 620 d postinoculation. The incubation period was calculated from the day of inoculation to the day of terminal clinical disease. Mice were maintained under specific pathogen-free conditions. All of the present studies were reviewed and approved by the animal care and use committee at the University of California, San Diego.

Sodium phosphotungstic acid (NaPTA) precipitation and Western blotting

Brain homogenates (10%) from all CWD-inoculated mice were subjected to NaPTA precipitation as described previously (28). In brief, brain extracts of ~ 1 mg of protein in PBS containing 2% sarcosyl were digested with an endonuclease (Benzonase; Sigma-Aldrich, St. Louis, MO, USA) followed by treatment with 50 μ g/ml proteinase K (PK) at 37°C for 30 min. After addition of NaPTA, MgCl₂, and protease inhibitors (Complete Protease Inhibitor; Roche, Indianapolis, IN, USA), extracts were incubated at 37°C for 30 min and centrifuged at 18,000 g for 30 min at 37°C. Pellets were resuspended in 0.1% sarcosyl. LDS loading buffer (Invitrogen, Grand Island, NY, USA) was then added, and samples were heated to 95°C before electrophoresis through a 10% Bis-Tris gel (Invitrogen) and transfer to a nitrocellulose membrane by wet blotting. Proteins were detected with anti-PrP antibody POM1 (epitope in the globular domain, aa 121-230, a kind gift from Dr. Adriano Aguzzi, Institute of Neuropathology, University Hospital Zurich, Zurich, Switzerland; ref. 29) followed by a horseradish peroxidase (HRP)-conjugated anti-mouse IgG antibody (Jackson ImmunoResearch Laboratories, West Grove, PA, USA). Signals were visualized using a chemiluminescent substrate (Supersignal West Dura; Thermo Fisher Scientific, Waltham, MA, USA) and an LAS-4000 imager (Fujifilm, Stamford, CT, USA). RML prion- and mock-infected brain samples were digested with PK and analyzed by Western blotting.

Detection of insoluble PrP

Brain homogenate samples were lysed in a Tris HCl-based buffer (10 mM Tris-HCl, pH 8.0, and 10 mM EDTA with 2% sarcosyl) and incubated at 37°C for 1 h before ultracentrifugation at 150,000 g for 1 h. The pellet fractions were collected and analyzed by Western blotting for PrP.

PrP peptide ELISA

The peptide ELISA was performed as described in Lau *et al.* (30) with minor modifications. Brain homogenate was mixed with an equal volume of lysis buffer (100 mM Tris-HCl, pH

7.5, and 150 mM NaCl) containing 2% sarcosyl and incubated for 20 min at 37°C. The samples were then incubated with peptide-coated magnetic beads (M-280; Invitrogen) for 1 h at 37°C with constant shaking. The beads were washed with TBS containing 0.1% Tween 20 before denaturation with 0.1 M NaOH and neutralization with 0.3 M NaH₂PO₄. PrP was then measured by standard sandwich ELISA using a 96-well plate precoated with 1.5 µg/ml POM-2 antibody and then using a biotinylated POM-1 antibody (50 ng/ml), followed by streptavidin-HRP (25 ng/ml) and a 1-Step Ultra TMB-ELISA substrate (Thermo Fisher Scientific) for detection. RML prion-infected and uninfected control brain samples were included in every experiment. Samples were run in triplicate.

Serial automated protein misfolding cyclic amplification (saPMCA)

Brain homogenates were prepared using mouse-adapted scrapie (RML), sheep scrapie (SSBP/1), mule deer CWD, and cattle BSE from the brains of clinically positive animals. The *in vitro* prion replication, including PrP^{Sc} detection of amplified samples, was performed following the basic conditions described previously (31). In brief, aliquots of 5 µl of 10% brain homogenate from animals infected by each prion strain were diluted into 50 µl of 10% previously perfused (5 mM EDTA in PBS) C57BL/6 WT and Tg(MoPrP^{167S}) brain homogenates and loaded into 0.2-ml PCR tubes. Mouse brain homogenates (10%, w/v) were prepared in conversion buffer (PBS containing 150 mM NaCl and 1% Triton X-100) with the addition of Complete Protease Inhibitor. Each prion strain was tested in triplicate. Tubes were positioned in an adaptor placed on the plate holder of a microsonicator (model S-4000MP1; QSonica, Newtown, CT, USA) and programmed to perform cycles of a 30-min incubation at 38°C followed by a 20-s pulse of sonication set at potency of 80-90. Samples were incubated without shaking in the water bath of the sonicator. Serial rounds of PMCA consisted of 27 h of standard PMCA followed by serial *in vitro* 1:10 passages in fresh mouse brain substrate. The detailed protocol for saPMCA, including reagents, solutions, and troubleshooting, has been published elsewhere (32).

The standard procedure to digest PrP^{Sc} was performed following the basic conditions described previously (33). In brief, 1 vol of amplified product was mixed with 1 vol of digestion buffer (PBS, 2% Tween, and 2% Nonidet P-40) and digested with PK (85 µg/µl) for 60 min at 42°C with shaking (450 rpm). Digestion was stopped by addition of 10 µl of SDS NuPAGE loading buffer and incubation at 100°C for 10 min. Proteins were fractionated by SDS-PAGE (12% gel; Invitrogen) and transferred onto nitrocellulose membranes. Membranes were incubated for 1 h with SAF-83 mAb (1:10,000; Cayman Chemical, Ann Arbor, MI, USA) followed by goat anti-mouse HRP. Immunoreactivity was detected using an enhanced chemiluminescent substrate (SuperSignal West Pico; Thermo Fisher Scientific). Western blot signals were analyzed using the FluorChem Q system and AlphaView Q software (Alpha Innotech, San Leandro, CA, USA).

Histopathology and immunohistochemical stains

Sections (2 µm thick) were cut onto positively charged silanized glass slides and stained with hematoxylin and eosin or immunostained using antibodies for PrP. For PrP staining, sections were deparaffinized and incubated for 5 min in 88% formic acid, then washed in water for 5 min, treated with 5 µg/ml of PK for 10 min, and washed in water for 5 min. Sections were then autoclaved in citrate buffer (pH 6) and cooled for 3 min. Immunohistochemical staining was per-

formed using the TSA Plus DNP kit (PerkinElmer Life and Analytical Sciences, Waltham, MA, USA). Sections were blocked and incubated with anti-PrP SAF-84 (1:400; Cayman Chemical) for 45 min, followed by anti-mouse HRP (1:500; Jackson ImmunoResearch Laboratories) for 30 min. Slides were then incubated with anti-dinitrophenyl-HRP (1:100; PerkinElmer Life and Analytical Sciences) for 30 min, followed by a 6-min incubation with 3,3'-diaminobenzidine substrate. Sections were counterstained with hematoxylin.

Luminescent conjugated polymer staining of tissue sections

The synthesis of polythiophene acetic acid (PTAA; mean molecular mass, 3 kDa) has been reported (34, 35). Frozen mouse brain sections were dried for 1 h and fixed in 100% ethanol for 10 min. After sections were washed with deionized water, they were equilibrated in PBS. Luminescent conjugated polymers were diluted in PBS (0.01 µg/µl), then added to the brain sections and incubated for 30 min at room temperature, and finally, the brain sections were washed with PBS.

Conformation stability assay

Stability of prions after guanidine hydrochloride (GdnHCl) denaturation was performed as described previously (36). In brief, brain homogenates in Tris lysis buffer (10 mM Tris-HCl, pH 7.4; 150 mM NaCl; and 2% sarcosyl) were mixed with an equal volume of GdnHCl stock solution and incubated for 1 h at room temperature. The samples were then diluted with lysis buffer to a final concentration of 0.15 M GdnHCl and digested with PK at a ratio of 1:500 (1 µg of PK:500 µg of total protein) for 1 h at 37°C. PK digestion was stopped with 3 mM PMSF and Complete Protease Inhibitor, and samples were centrifuged at 18,000 g for 1 h at 4°C. The pellets were washed with 500 µl of 0.1 M NaHCO₃ (pH 9.6) and centrifuged for 20 min at 18,000 g. Pellets were resuspended in 6 M guanidine thiocyanate for 20 min and diluted 2-fold with 0.1 M NaHCO₃. Proteins were passively coated onto an ELISA plate. PrP was detected with anti-PrP biotinylated-POM1 antibody and streptavidin-HRP-conjugated anti-mouse IgG secondary antibody. The signals were detected with a chemiluminescent substrate (1-Step Ultra TMB-ELISA). Denaturation curves were plotted as PrP^{Sc} absorbance signals against the GdnHCl concentration and fitted to a sigmoid function (variable slope). [GdnHCl]_{1/2} values for mice expressing MoPrP or MoPrP^{167S} infected with RML mouse prions were calculated with each mouse as an individual data point, which was the average signal for samples run in triplicate. [GdnHCl]_{1/2} values were expressed as the log EC₅₀ using GraphPad Prism 5.0 (GraphPad Software Inc., San Diego, CA, USA). Between 5 and 7 mice were analyzed for each *Prnp* genotype (mouse PrP or PrP^{167S}). Statistical analysis was performed using an unpaired, 2-tailed Student's *t* test.

Cell culture studies of PrP with amino acid exchanges at residue 167

CAD-RML cells were transfected with plasmid pcDNA 3.1 encoding PrP using Lipofectamine. Cells were lysed at 45–48 h posttransfection using a Tris-based lysis buffer containing 0.5% Nonidet P-40 and 0.5% deoxycholate. Cell lysates containing 60–80 µg of protein were digested with 5 µg/ml PK for 30 min at 37°C and analyzed along with 15–20 µg of protein from undigested samples by SDS-PAGE. Immunoblotting was initially performed using the anti-PrP antibody, 3F4, followed by immunoblotting using the anti-PrP antibody POM1 and anti-actin antibody. Signals were captured and quantified using a Fujifilm

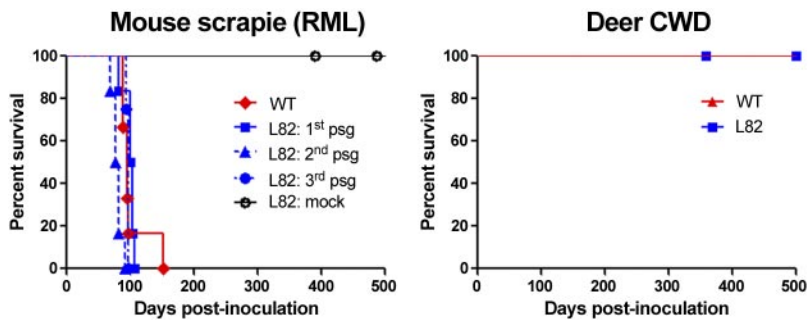


Figure 1. The RL structure has no effect on transmission barriers to mouse or deer prions in *Tg(MoPrP^{167S})* mice. **A**) Survival curves for WT and *Tg(MoPrP^{167S})82* (L82) mice, inoculated with RML mouse-adapted scrapie. *Tg(MoPrP^{167S})*-RML was passaged 3 times, and all mice developed clinical prion disease. **B**) Survival curves for WT and *Tg(MoPrP^{167S})82* mice inoculated with CWD deer prions. At 500 d postinoculation, no clinical signs of prion disease were noted in any CWD-inoculated mice.

LAS-4000 imager and Multigage software. The ratio of PK-resistant PrP to total PrP was calculated. Five (RL) or 8 (167 mutation) experimental replicates were performed.

RESULTS

WT and *Tg(MoPrP^{167S})* mice are highly susceptible to mouse prions and showed no detectable infection after exposure to deer prions

We first assessed prion conversion in mice expressing PrP^C sequences that vary by one residue in the β 2- α 2 loop using 1) WT mice, which express PrP^C with a disordered loop, and 2) transgenic mice, which express mouse PrP^C with a RL due to a D167S substitution [*Tg(MoPrP^{167S})*]. *Tg(MoPrP^{167S})* mice from line 82 were propagated because mice express low (1- to 2-fold WT) levels of PrP^C (26). We inoculated WT and *Tg(MoPrP^{167S})82* mice with RML prions from mice. The *Tg(MoPrP^{167S})82* mice developed prion disease with clinical signs of severe ataxia, kyphosis, stiff tail, and weight loss at time points similar to

those of WT mice [99 ± 4 d in *Tg(MoPrP^{167S})* mice *vs.* 103 ± 4 d in WT mice], suggesting that the RL structure had no influence on RML prion conversion (**Fig. 1A**).

Evidence of transmission barriers can also be detected during serial passage whereby the incubation period shortens. Therefore, we performed second and third passages of RML-MoPrP^{167S}. The *Tg(MoPrP^{167S})82* mice developed prion disease with a similar incubation period at each passage, suggesting that there was no transmission barrier for RML prions (Fig. 1A). We performed a PK digestion and immunoblotting on *Tg(MoPrP^{167S})82* brain samples and readily detected PK-resistant PrP^{Sc} in mice from all three passages (**Fig. 2A**).

Deer express PrP^C with an ordered RL due to the 170N and 174T residues. We inoculated known infectious CWD prions from deer into WT and *Tg(MoPrP^{167S})82* mice. No mice developed clinical signs of prion infection (Fig. 1B). In addition, no PrP^{Sc} was detected in WT or *Tg(MoPrP^{167S})82* mice after NaPTA precipitation and immunoblotting (Fig. 2B) or by immunohistochemical analysis for PrP in brain sections (data not shown). To further test whether

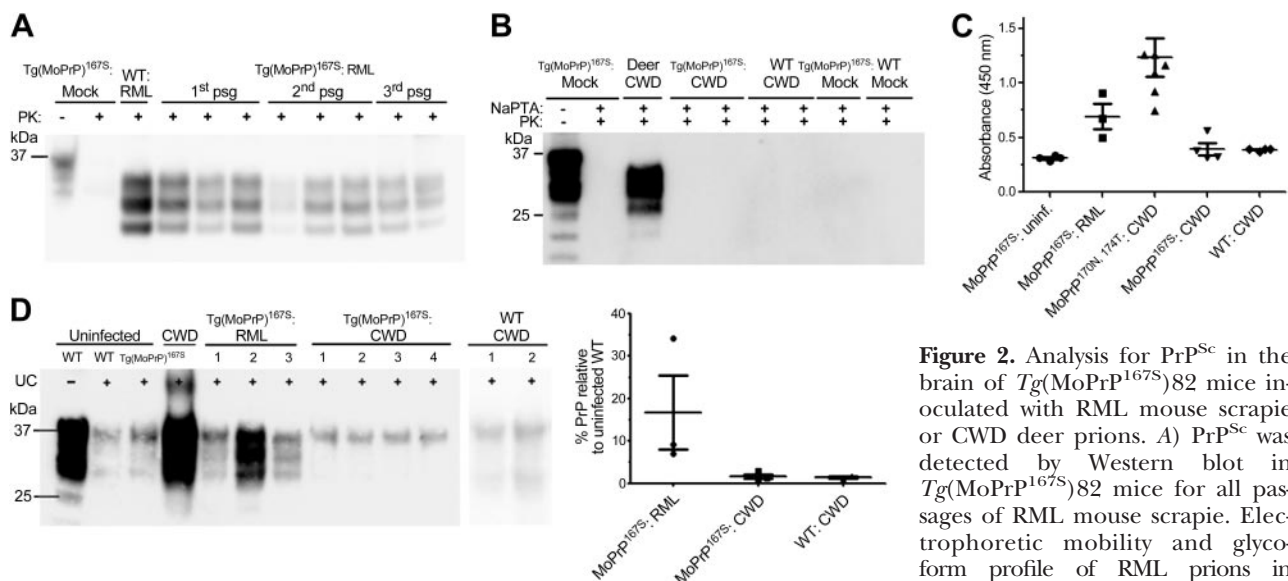


Figure 2. Analysis for PrP^{Sc} in the brain of *Tg(MoPrP^{167S})82* mice inoculated with RML mouse scrapie or CWD deer prions. **A**) PrP^{Sc} was detected by Western blot in *Tg(MoPrP^{167S})82* mice for all passages of RML mouse scrapie. Electrophoretic mobility and glycoform profile of RML prions in

Tg(MoPrP^{167S})82 mice from all passages is similar to that of RML prions in WT mice. **B**) Representative blot shows that no PrP^{Sc} was detected in the *Tg(MoPrP^{167S})82* or WT mice inoculated with CWD after NaPTA precipitation. **C**) Likewise, no aggregated PrP was detected in *Tg(MoPrP^{167S})* or WT mice inoculated with CWD by PrP peptide ELISA, whereas PrP aggregates were detectable in RML prion-inoculated *Tg(MoPrP^{167S})* mice and in CWD prion-inoculated *Tg(MoPrP^{170N,174T})* mice. **D**) Insoluble fraction of brain homogenate from RML- and CWD-prion inoculated *Tg(MoPrP^{167S})* mice after ultracentrifugation (UC) shows little insoluble PrP in the CWD prion-inoculated *Tg(MoPrP^{167S})* or WT mice, yet high levels in RML prion-inoculated *Tg(MoPrP^{167S})* mice. Numbers correspond to different individual mice. The PrP signal was quantified, and levels relative to uninfected WT samples were plotted.

TABLE 1. Amino acid sequence at the $\beta 2\text{-}\alpha 2$ loop of PrP^C and in vivo barrier to prion conversion

PrP construct expressed in transgenic mice	Primary sequence 167–175	Secondary structure of $\beta 2\text{-}\alpha 2$ loop	Transmission barrier to RML mouse prions	Transmission barrier to CWD deer prions
MoPrP	DQYSNQNNF	Disordered	No	Yes
MoPrP ^{167S}	SQYSNQNNF	Ordered, rigid	No	Yes
MoPrP ^{170N,174T^a}	DQYNNQNTF	Ordered, rigid	Yes	Yes ^b
CerPrP ^a	DQYNNQNTF	Ordered, rigid	Yes	No

^aThe transmission barriers were described previously (24, 39). ^bAll mice developed prion disease <400 d after inoculation, whereas mice expressing MoPrP or MoPrP^{167S} required >400 d after inoculation to develop CWD-induced prion disease or resisted CWD infection.

PrP^{Sc} could be detected using highly sensitive assays without the use of PK, we performed PrP peptide precipitation and ELISA (30). Again we were not able to detect PrP^{Sc} in CWD-inoculated *Tg*(MoPrP^{167S})82 or WT brains (Fig. 2C). In addition, we performed ultracentrifugation of brain homogenate and measured the amount of insoluble PrP in the pellet fraction. Abundant insoluble PrP was detected in RML prion-inoculated *Tg*(MoPrP^{167S})82 mice, but only at background levels in the CWD-inoculated *Tg*(MoPrP^{167S})82 and WT mice comparable to levels in uninfected mice (Fig. 2D). The identical CWD-infected brain homogenate has been shown to be infectious to *Tga*20 mice (>400–600 dpi) and to *Tg*1020 mice (>220 dpi) in two previous studies (24, 27). Thus, overall the transmission barriers for the *Tg*(MoPrP^{167S}) mice expressing RL PrP exactly matched that of mice expressing flexible loop MoPrP (Table 1).

Mouse PrP and MoPrP^{167S} PrP conversion efficiency on seeding with prions from 5 species in the PMCA assay

Our initial results using mouse and deer prions indicated that the transmission barriers were not altered by the D167S substitution. To further investigate the transmission barrier, we used PMCA, which has been shown to successfully mimic species barriers reported *in vivo* (37–39). Here, using brain homogenate from WT and *Tg*(MoPrP^{167S})82 mice as substrates for PrP^C, we seeded the PMCA reaction with prions from hamsters, cattle, sheep, mice, and deer. Three separate replicate samples were seeded with each strain and amplified for 4 to 5 rounds, using 27 cycles of sonication and a 1:10 dilution into fresh substrate with each subsequent round. Here again we found no differences in prion species barriers caused by the single D167S residue substitution (Fig. 3). Both mouse and *Tg*(MoPrP^{167S})82 substrate successfully amplified seeds from mouse and bovine prions, yet did not amplify prions from hamster, sheep, or deer (Table 2). In contrast, deer, sheep, and hamster substrate supported efficient amplification of hamster, sheep, and deer prions (data not shown).

Substitution of other residues at position 167 does not affect conversion with RML prions

To further exclude the possibility that the D167S substitution has led to barriers to prion conversion, we used a persistently RML prion-infected CAD neuronal cell line (40) expressing the D167S variant. The WT

PrP^C and D167S variant contained the 3F4 epitope tag (L109M, V112M) to distinguish the PrP from endogenous WT mouse RML prions. Constructs were transfected into RML prion-infected CAD cells, cells were lysed after 45–48 h, and the amount of PrP converted was measured by PK digestion followed by immunoblotting with an antibody against the 3F4 epitope tag. We found that the WT PrP^C and D167S variant were converted in the RML prion-infected cells, indicating that the single substitution had little effect on transmission efficiency (Fig. 4A).

To investigate whether any other residue substitutions at position 167 would affect RML prion conversion, we expressed 3F4 epitope-tagged mouse PrP^C with three additional residue substitutions at position 167: alanine, glycine, and glutamate. Interestingly, we found that all constructs were converted by RML prions at levels similar to or slightly less than those for the WT-3F4 PrP^C (Fig. 4). However, PrP^C with the original RL substitutions, 170N

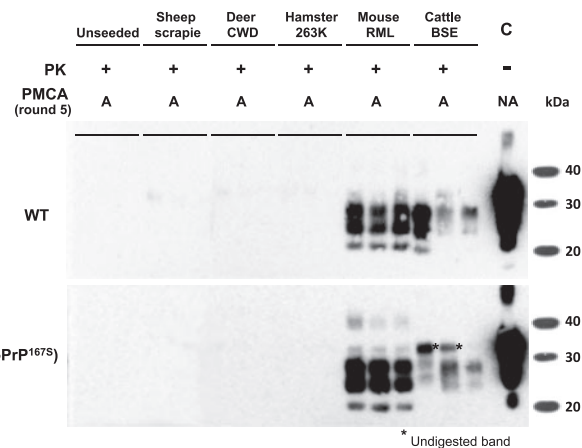


Figure 3. Biochemical analysis of different samples generated *in vitro* by saPMCA using WT or *Tg*(MoPrP^{167S})82 brain homogenates as substrate. WT and *Tg*(MoPrP^{167S})82 brain homogenates seeded with different prion strains (mouse, RML; mule deer, CWD; cattle, BSE; hamster, 263K; and sheep, SSBP/1) or left unseeded were subjected to saPMCA. Seeded samples from round 5 were digested with 85 μ g/ml of PK and analyzed by Western blot using monoclonal antibody SAF83. Almost identical amplification of mouse and cattle prions but not of hamster, sheep, or deer prions occurred with both substrates. Unseeded samples used as PMCA negative controls did not show any PK-resistant PrP band in any of the PMCA rounds performed. A, *in vitro* amplified sample; NA, nonamplified sample; C, control non-PK-digested normal mouse brain homogenate.

TABLE 2. Automated serial PMCA using WT or *Tg(MoPrP^{167S})* brain homogenate as the substrate

PrP ^C source	Experiment 1 (4 rounds)	Experiment 2 (5 rounds)
Unseeded		
WT	0/3	0/3
<i>Tg(MoPrP^{167S})</i>	0/3	0/3
Sheep (SSBP1)		
WT	0/3	0/3
<i>Tg(MoPrP^{167S})</i>	0/3	0/3
Deer CWD		
WT	0/3	0/3
<i>Tg(MoPrP^{167S})</i>	0/3	0/3
Hamster (263K)		
WT	0/3	0/3
<i>Tg(MoPrP^{167S})</i>	0/3	0/3
Mouse (RML)		
WT	3/3	3/3
<i>Tg(MoPrP^{167S})</i>	3/3	3/3
Cattle BSE		
WT	1/3	3/3
<i>Tg(MoPrP^{167S})</i>	1/3	2/3

Brains from WT and *Tg(MoPrP^{167S})* mice were extracted after perfusion with PBS + 5 mM EDTA and used as substrate or source of PrP^C. Brain homogenates (60 μ l) were treated in replicates of 3 ($n=3$) with saPMCA and were incubated-sonicated for 27 h in each round. After each round of PMCA, the PK-resistant PrP (PrP^{Sc}) in the incubated-sonicated samples was diluted 1:10 into a freshly prepared WT and *Tg(MoPrP^{167S})* mouse brain homogenate to start the next PMCA round. This process was repeated for 4 or 5 rounds (P5). The fraction of PrP^{Sc}-positive tubes is indicated.

and N174T, was poorly converted by mouse prions (Fig. 4), consistent with our previously reported results using *in vivo* mouse models and PMCA (24).

D167S substitution alters the plaque morphology and PTAA emission spectra of RML mouse prions

Having shown no apparent transmission barrier to mouse prions in the *Tg(MoPrP^{167S})* mice, we hypothesized that the

brain histopathology and biochemical properties would be identical in WT and *Tg(MoPrP^{167S})* mice. To test this hypothesis, we next assessed the PrP^{Sc} aggregate morphology and PTAA binding in the brains of RML prion-infected WT and *Tg(MoPrP^{167S})* mice. Surprisingly, there were subtle changes in the plaque morphology in the PrP-immunostained brain sections. The *Tg(MoPrP^{167S})*82 mice developed slightly larger and more dense plaques than the WT mice (Fig. 5A).

PTAA binds amyloid and has been used to distinguish prion strains (41). PTAA does not typically bind to RML aggregates in tissue sections (41). We found no binding of PTAA to RML prions in WT mice brain sections as reported previously, yet PTAA did bind to a subpopulation of the MoPrP^{167S}-RML aggregates in all passages in mice from line 82 (Fig. 5B). Together these findings suggest that although RML prion transmission was efficient, the resulting PrP^{Sc} conformation of the MoPrP^{167S}-RML differed.

Conformational stability of MoPrP^{167S}-RML differs from that of WT-RML

We assessed whether biochemical differences could be detected between the RML prions in WT and *Tg(MoPrP^{167S})* mice. We found no significant differences in the PK-resistant PrP^{Sc} core size or the glycoform ratios of PrP in the brains of MoPrP-RML- and MoPrP^{167S}-RML-infected mice (Fig. 2 and Supplemental Fig. S1).

To test whether differences had developed in the PrP^{Sc} conformational stability in the 167S RML variant, we exposed aliquots of RML-infected brain homogenate to 14 concentrations of GdnHCl, digested samples with PK, and measured the PrP^{Sc} remaining by ELISA. Overall, the stability of the MoPrP^{167S}-RML was modestly but significantly increased compared with that of the MoPrP-RML (MoPrP^{167S} 1.2 ± 0.06 vs. MoPrP 0.95 ± 0.03 ; $P=0.006$, unpaired, 2-tailed Student's *t* test; Fig. 6). The ability of MoPrP^{167S} aggregates to bind to PTAA, together with the

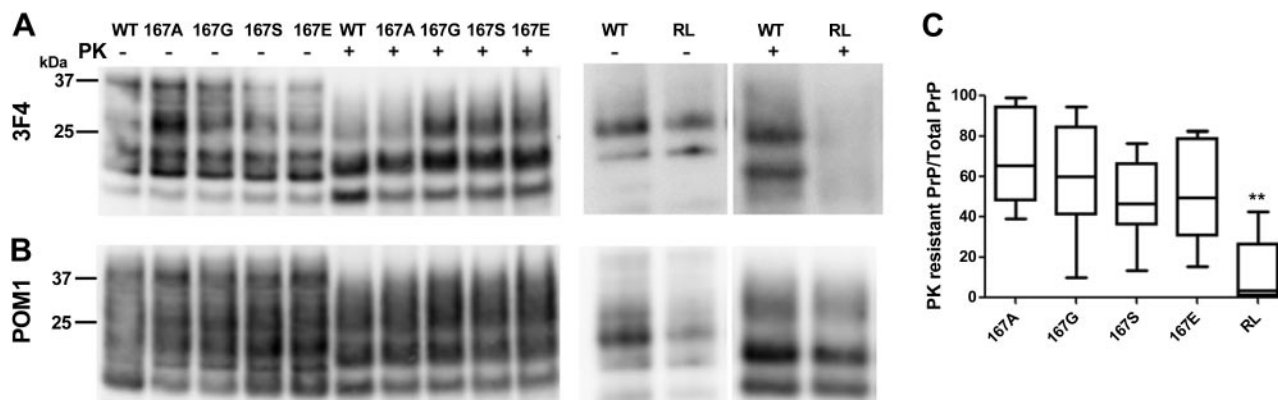


Figure 4. RML mouse prions in immortalized CAD cells efficiently convert mouse PrP^C with amino acid substitutions at position 167. A) Western blot shows that the 3F4 epitope-tagged PrP^{Sc} from WT and 167 mutants (167A, 167G, 167S, and 167E) are efficiently converted by the RML prions, whereas the RL mutant with the 170N, 174T substitutions is poorly converted. B) Membrane from panel A immunoblotted with anti-PrP antibody POM1 shows that the endogenous PrP^{Sc} levels are unaffected by the PrP^{Sc} mutants. C) Ratio of PK-digested PrP^{Sc} to total PrP signal relative to WT (normalized to an upper limit of 1.0). There was no significant difference ($P<0.01$) between WT PrP and the 167 PrP mutants when the raw values were compared. There was a significant difference between the WT and RL mutant (170N, 174T) in a Student's *t* test. $**P < 0.001$.

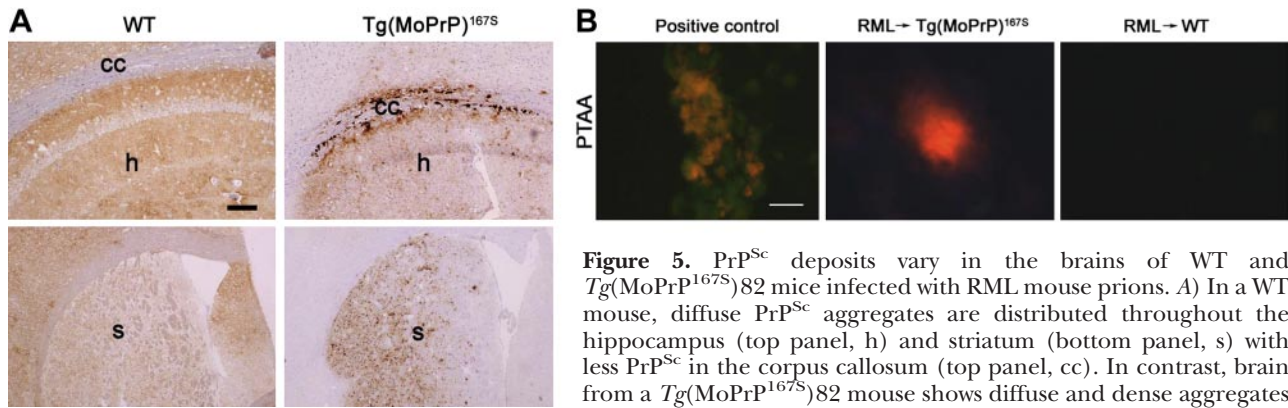


Figure 5. PrP^{Sc} deposits vary in the brains of WT and Tg(MoPrP^{167S})82 mice infected with RML mouse prions. A) In a WT mouse, diffuse PrP^{Sc} aggregates are distributed throughout the hippocampus (top panel, h) and striatum (bottom panel, s) with less PrP^{Sc} in the corpus callosum (top panel, cc). In contrast, brain from a Tg(MoPrP^{167S})82 mouse shows diffuse and dense aggregates in the hippocampus and corpus callosum (top panel) and dense punctuate aggregates in the striatum. B) Only RML prion-infected Tg(MoPrP^{167S})82 mice developed plaques that bind PTAA. Positive control is from an RML prion-infected transgenic mouse expressing glycosylphosphatidylinositol-anchorless PrP. Scale bars = 200 μ m (A); 15 μ m (B).

punctuate aggregates in the striatum. B) Only RML prion-infected Tg(MoPrP^{167S})82 mice developed plaques that bind PTAA. Positive control is from an RML prion-infected transgenic mouse expressing glycosylphosphatidylinositol-anchorless PrP. Scale bars = 200 μ m (A); 15 μ m (B).

increased conformational stability, suggests that the RML conformation is modified in the MoPrP^{167S} variant.

DISCUSSION

β 2- α 2 loop homology and cross-species prion conversion

Barriers to interspecies prion transmission are due in part to structural differences between PrP^C and PrP^{Sc}, and even variation of one residue can inhibit prion conversion (12). Key residue differences in the unstructured N-terminal region or the globular C-terminal domain can interfere with prion conversion experimentally (42–45), yet how secondary structural changes influence prion conversion is unknown. Here, using rationally designed modifications of mouse PrP structure, the effect of a primary and secondary structural change on interspecies prion transmission could be uncoupled.

In earlier work, we showed that transgenic mice expressing mouse PrP or mouse PrP with the S170N and N174T substitutions, which result in a rigid β 2- α 2 loop, show profound differences in cross-species prion suscep-

tibility (24). Only the Tg(MoPrP^{170N,174T}) mice were highly susceptible to hamster and deer prions, which share the rigid β 2- α 2 loop as well as the 170 asparagine.

In the present study, we assess species barriers using transgenic mice that express PrP^C with a rigid β 2- α 2 loop due to a D167S substitution. Through testing prion susceptibility of transgenic mice and through PMCA experiments of MoPrP^{167S}, we show poor or no conversion of infectious prions from species having a RL, indicating that the common RL structure provided no advantage in conversion efficiency. Mice expressing PrP with a disordered (WT) or an ordered (MoPrP^{167S}) loop showed no difference in transmission barriers. Consistent with these findings, persistently prion-infected CAD cells expressing mutant PrP^C showed that residue exchanges at position 167 had little effect on prion conversion. The overall homology of the amino acid sequence of the β 2- α 2 loop between host PrP^C and incoming PrP^{Sc} influenced prion conversion. Thus, taken together, the results of the D167S substitution provide a deeper understanding of the earlier transmission studies and indicate that the sequence homology at residue 170, and not the RL structure,

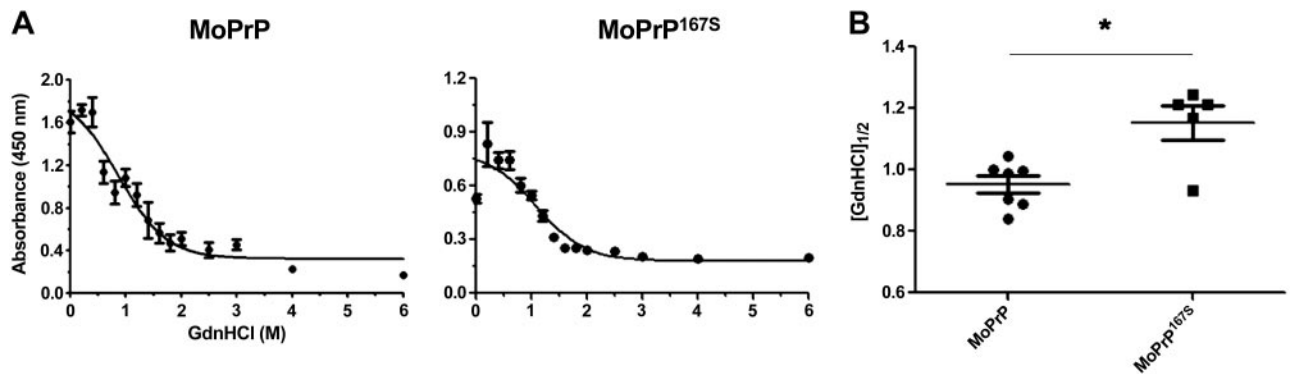


Figure 6. Conformational stability of RML prions in mice expressing MoPrP or MoPrP^{167S}. A) Brain homogenate was denatured with increasing concentrations of GdnHCl and partially digested with PK. PrP^{Sc} was detected by ELISA. Denaturation curves were plotted as PrP^{Sc} absorbance signals against the GdnHCl concentration and fitted to a sigmoid function. Half-maximal denaturation occurred at GdnHCl concentrations that were greater for MoPrP^{167S}-RML than for MoPrP-RML. B) Plot of [GdnHCl]_{1/2} values for mice expressing MoPrP or MoPrP^{167S} infected with RML mouse prions showing each mouse as an individual data point, which is the average signal for samples run in triplicate. **P* < 0.01.

enabled CWD- and hamster scrapie-driven conversion described in the *Tg*(MoPrP^{170N,174T}) mice.

The importance of the primary sequence in mammalian PrP conversion is consistent with yeast prion studies, which have elegantly shown that small stretches of the primary sequence underlie the intermolecular contacts required for conversion (reviewed in ref. 46). These short recognition sequences control prion propagation and may vary, depending on the strain (47, 48). Similar to mammalian PrP, single-residue substitutions at key sites in a yeast prion can alter the prion strain (49) as well as alter critical steps in prion propagation, such as aggregate delivery to daughter cells (50).

Mouse-adapted prions efficiently convert the MoPrP^{167S} variant and modify the PrP^{Sc} conformational properties

Heterologous PrP^C and PrP^{Sc} sequences can lead to inefficient prion conversion and prolonged incubation periods in rodent models (51). In addition, the brain regions targeted, aggregate morphology, and PrP^{Sc} conformational properties may also be modified. Subsequent serial passage through the variant sequence typically leads to a reduced and more consistent incubation period (52). Here we show that despite no significant difference in the incubation period on initial or subsequent passage of RML mouse prions in *Tg*(MoPrP)^{167S} mice, the PrP^{Sc} conformational properties have changed remarkably from RML prions, as indicated by the binding of PTAA to plaques and the increased PrP^{Sc} stability after exposure to chaotropes. These results indicate that the PrP^{Sc} assemblies were modified on transmission through a heterologous sequence, although prion conversion remained highly efficient.

How might the β 2- α 2 loop sequence affect the PrP^{Sc} structure at the atomic level? Because atomic level crystal structures of β 2- α 2 loop peptides have shown that loop peptides form a steric zipper structure (19), substituting a residue may alter the side chain packing arrangement of the β -sheet interface or the range of available packing arrangements (20). Thus, the conformational differences in prions caused by 1 to 2 residue exchanges in the β 2- α 2 loop might be akin to the variation observed among certain steric zippers (20).

Taken together, these findings underscore the key role of homology of the primary sequence at certain critical residues, such as 170N, in cross-species prion transmission and in prion conformation. The interacting recognition sequences between PrP^C and PrP^{Sc} may be determined by the incoming PrP^{Sc} conformation. Identifying the interacting residues for particular prion conformations may enable better predictions of cross-species prion transmission as well as potential targets for therapeutic intervention. **FJ**

The authors thank Dr. Adriano Aguzzi (Institute of Neuropathology, University Hospital Zurich, Zurich, Switzerland) and Dr. Charles Weissmann (The Scripps Research Institute Florida, Jupiter, FL, USA) for kindly providing the anti-PrP POM antibodies and the CAD-RML cells, respectively; Mona Farahi, Rozalyn Simon, and Karin Magnusson for excellent technical support; and Drs. David Eisenberg and Michael Sawaya for helpful discussions. The authors also thank the animal caretakers at the University of California, San Diego,

and CIC bioGUNE and Drs. Jean E. Jewell (University of Wyoming, Laramie, WY, USA) and Tomás Mayoral (Central Veterinary Laboratory, Madrid, Spain) for the CWD and BSE brain samples. This study was supported by the U.S. National Institutes of Health (NS055116, NS069566, and U54AI0359; C.J.S.); a national grant from Spain (AGL2009-11553-C02-01); a Basque government grant (PI2010-18); the IKERBasque Foundation; the Department of Industry, Tourism, and Trade of the Government of the Autonomous Community of the Basque Country (Etorrek Research Programs 2011/2013); the Innovation Technology Department of Bizkaia County; and an Institutional Grant for Younger Researchers from the Swedish Foundation for International Cooperation in Research and Higher Education (STINT; C.J.S., K.P.R.N.).

REFERENCES

1. Wells, G. A., and Wilesmith, J. W. (1995) The neuropathology and epidemiology of bovine spongiform encephalopathy. *Brain Pathol.* **5**, 91–103
2. Prusiner, S. B. (1982) Novel proteinaceous infectious particles cause scrapie. *Science* **216**, 136–144
3. Prusiner, S. B. (1991) Molecular biology of prion diseases. *Science* **252**, 1515–1522
4. Will, R. G., Ironside, J. W., Zeidler, M., Cousens, S. N., Estibeiro, K., Alperovitch, A., Poser, S., Pocchiari, M., Hofman, A., and Smith, P. G. (1996) A new variant of Creutzfeldt-Jakob disease in the UK. *Lancet* **347**, 921–925
5. Collinge, J., Sidle, K. C., Meads, J., Ironside, J., and Hill, A. F. (1996) Molecular analysis of prion strain variation and the aetiology of 'new variant' CJD. *Nature* **383**, 685–690
6. Bruce, M. E., Will, R. G., Ironside, J. W., McConnell, I., Drummond, D., Suttie, A., McCordle, L., Chree, A., Hope, J., Birkett, C., Cousens, S., Fraser, H., and Bostock, C. J. (1997) Transmissions to mice indicate that 'new variant' CJD is caused by the BSE agent *Nature* **389**, 498–501
7. Kirkwood, J. K., Cunningham, A. A., Wells, G. A., Wilesmith, J. W., and Barnett, J. E. (1993) Spongiform encephalopathy in a herd of greater kudu (*Tragelaphus strepsiceros*): epidemiological observations. *Vet. Rec.* **133**, 360–364
8. Kirkwood, J. K., and Cunningham, A. A. (1994) Epidemiological observations on spongiform encephalopathies in captive wild animals in the British Isles. *Vet. Rec.* **135**, 296–303
9. Ryder, S. J., Wells, G. A., Bradshaw, J. M., and Pearson, G. R. (2001) Inconsistent detection of PrP in extraneural tissues of cats with feline spongiform encephalopathy. *Vet. Rec.* **148**, 437–441
10. Piening, N., Nonno, R., Di Bari, M., Walter, S., Windl, O., Agrimi, U., Kretzschmar, H. A., and Bertsch, U. (2006) Conversion efficiency of bank vole prion protein *in vitro* is determined by residues 155 and 170, but does not correlate with the high susceptibility of bank voles to sheep scrapie *in vivo*. *J. Biol. Chem.* **281**, 9373–9384
11. Barron, R. M., Thomson, V., Jamieson, E., Melton, D. W., Ironside, J., Will, R., and Manson, J. C. (2001) Changing a single amino acid in the N-terminus of murine PrP alters TSE incubation time across three species barriers. *EMBO J.* **20**, 5070–5078
12. Priola, S. A., and Chesebro, B. (1995) A single hamster PrP amino acid blocks conversion to protease-resistant PrP in scrapie-infected mouse neuroblastoma cells. *J. Virol.* **69**, 7754–7758
13. Riek, R., Hornemann, S., Wider, G., Billeter, M., Glockshuber, R., and Wüthrich, K. (1996) NMR structure of the mouse prion protein domain PrP(121–321). *Nature* **382**, 180–182
14. Riek, R., Hornemann, S., Wider, G., Glockshuber, R., and Wüthrich, K. (1997) NMR characterization of the full-length recombinant murine prion protein, mPrP(23–231). *FEBS Lett.* **413**, 282–288
15. Schatzl, H. M., Da Costa, M., Taylor, L., Cohen, F. E., and Prusiner, S. B. (1997) Prion protein gene variation among primates. *J. Mol. Biol.* **265**, 257
16. Billeter, M., Riek, R., Wider, G., Hornemann, S., Glockshuber, R., and Wüthrich, K. (1997) Prion protein NMR structure and species barrier for prion diseases. *Proc. Natl. Acad. Sci. U. S. A.* **94**, 7281–7285

17. Christen, B., Perez, D. R., Hornemann, S., and Wüthrich, K. (2008) NMR structure of the bank vole prion protein at 20 °C contains a structured loop of residues 165–171. *J. Mol. Biol.* **383**, 306–312
18. Gossert, A. D., Bonjour, S., Lysek, D. A., Fiorito, F., and Wüthrich, K. (2005) Prion protein NMR structures of elk and of mouse/elk hybrids. *Proc. Natl. Acad. Sci. U. S. A.* **102**, 646–650
19. Sawaya, M. R., Sambashivan, S., Nelson, R., Ivanova, M. I., Sievers, S. A., Apostol, M. I., Thompson, M. J., Balbirnie, M., Wiltzius, J. J., McFarlane, H. T., Madsen, A. O., Riek, C., and Eisenberg, D. (2007) Atomic structures of amyloid cross- β spines reveal varied steric zippers. *Nature* **447**, 453–457
20. Wiltzius, J. J., Landau, M., Nelson, R., Sawaya, M. R., Apostol, M. I., Goldschmidt, L., Soriaga, A. B., Cascio, D., Rajashankar, K., and Eisenberg, D. (2009) Molecular mechanisms for protein-encoded inheritance. *Nat. Struct. Mol. Biol.* **16**, 973–978
21. Kaneko, K., Zulianello, L., Scott, M., Cooper, C. M., Wallace, A. C., James, T. L., Cohen, F. E., and Prusiner, S. B. (1997) Evidence for protein X binding to a discontinuous epitope on the cellular prion protein during scrapie prion propagation. *Proc. Natl. Acad. Sci. U. S. A.* **94**, 10069–10074
22. Kurt, T. D., Telling, G. T., Zabel, M. D., Hoover, E. A. (2009) Trans-species amplification of PrPCWD and correlation with rigid loop 170N. *Virology* **387**, 235–243
23. Kurt, T. D., Seelig, D. M., Schneider, J. R., Johnson, C. J., Telling, G. C., Heisey, D. M., and Hoover, E. A. Alteration of the chronic wasting disease species barrier by *in vitro* prion amplification. *J. Virol.* **85**, 8528–8537
24. Sigurdson, C. J., Nilsson, K. P., Hornemann, S., Manco, G., Fernandez-Borges, N., Schwarz, P., Castilla, J., Wüthrich, K., and Aguzzi, A. (2010) A molecular switch controls interspecies prion disease transmission in mice. *J. Clin. Invest.* **120**, 2590–2599
25. Perez, D. R., Damberger, F. F., and Wüthrich, K. (2010) Horse prion protein NMR structure and comparisons with related variants of the mouse prion protein. *J. Mol. Biol.* **400**, 121–128
26. Sigurdson, C. J., Joshi-Barr, S., Bett, C., Winson, O., Manco, G., Schwarz, P., Rulicke, T., Nilsson, K. P., Margalith, I., Raeber, A., Peretz, D., Hornemann, S., Wüthrich, K., and Aguzzi, A. (2011) Spongiform encephalopathy in transgenic mice expressing a point mutation in the β 2- α 2 loop of the prion protein. *J. Neurosci.* **31**, 13840–13847
27. Sigurdson, C. J., Manco, G., Schwarz, P., Liberski, P., Hoover, E. A., Hornemann, S., Polymenidou, M., Miller, M. W., Glatzel, M., and Aguzzi, A. (2006) Strain fidelity of chronic wasting disease upon murine adaptation. *J. Virol.* **80**, 12303–12311
28. Wadsworth, J. D. F., Joiner, S., Hill, A. F., Campbell, T. A., Desbruslais, M., Luthert, P. J., Collinge, J. (2001) Tissue distribution of protease resistant prion protein in variant CJD using a highly sensitive immuno-blotting assay. *Lancet* **358**, 171–180
29. Polymenidou, M., Moos, R., Scott, M., Sigurdson, C., Shi, Y. Z., Yajima, B., Hafner-Bratkovic, I., Jerala, R., Hornemann, S., Wüthrich, K., Bellon, A., Vey, M., Garen, G., James, M. N., Kav, N., and Aguzzi, A. (2008) The POM monoclonals: a comprehensive set of antibodies to non-overlapping prion protein epitopes. *PLoS ONE* **3**, e3872
30. Lau, A. L., Yam, A. Y., Michelitsch, M. M., Wang, X., Gao, C., Goodson, R. J., Shimizu, R., Timoteo, G., Hall, J., Medina-Selby, A., Coit, D., McCoin, C., Phelps, B., Wu, P., Hu, C., Chien, D., and Peretz, D. (2007) Characterization of prion protein (PrP)-derived peptides that discriminate full-length PrP^{Sc} from PrP^C. *Proc. Natl. Acad. Sci. U. S. A.* **104**, 11551–11556
31. Castilla, J., Saa, P., Morales, R., Abid, K., Maundrell, K., and Soto, C. (2006) Protein misfolding cyclic amplification for diagnosis and prion propagation studies. *Methods Enzymol.* **412**, 3–21
32. Saa, P., Castilla, J., and Soto, C. (2005) Cyclic amplification of protein misfolding and aggregation. *Methods Mol. Biol.* **299**, 53–65
33. Castilla, J., Saa, P., Hetz, C., and Soto, C. (2005) *In vitro* generation of infectious scrapie prions. *Cell* **121**, 195–206
34. Ding, L., Jonforsen, M., Roman, L. S., Andersson, M. R., and Inganas, O. (2000) Photovoltaic cells with a conjugated polyelectrolyte. *Synth. Met.* **110**, 133–140
35. Ho, H.-A., Boissinot, M., Bergeron, M. G., Corbeil, G., Dore, K., Boudreau, D., and Leclerc, M. (2002) Colorimetric and fluorometric detection of nucleic acids using cationic polythiophene derivatives. *Angew. Chem. Int. Ed. Engl.* **41**, 1548–1551
36. Peretz, D., Williamson, R. A., Legname, G., Matsunaga, Y., Vergara, J., Burton, D. R., DeArmond, S. J., Prusiner, S. B., and Scott, M. R. (2002) A change in the conformation of prions accompanies the emergence of a new prion strain. *Neuron* **34**, 921–932
37. Castilla, J., Morales, R., Saa, P., Barria, M., Gambetti, P., and Soto, C. (2008) Cell-free propagation of prion strains. *EMBO J.* **27**, 2557–2566
38. Castilla, J., Gonzalez-Romero, D., Saa, P., Morales, R., De Castro, J., and Soto, C. (2008) Crossing the species barrier by PrP(Sc) replication *in vitro* generates unique infectious prions. *Cell* **134**, 757–768
39. Green, K. M., Castilla, J., Seward, T. S., Napier, D. L., Jewell, J. E., Soto, C., and Telling, G. C. (2008) Accelerated high fidelity prion amplification within and across prion species barriers. *PLoS Pathog.* **4**, e1000139
40. Qi, Y., Wang, J. K., McMillian, M., and Chikaraishi, D. M. (1997) Characterization of a CNS cell line, CAD, in which morphological differentiation is initiated by serum deprivation. *J. Neurosci.* **17**, 1217–1225
41. Sigurdson, C. J., Nilsson, K. P., Hornemann, S., Manco, G., Polymenidou, M., Schwarz, P., Leclerc, M., Hammarstrom, P., Wüthrich, K., and Aguzzi, A. (2007) Prion strain discrimination using luminescent conjugated polymers. *Nat. Methods* **4**, 1023–1030
42. Scott, M., Groth, D., Foster, D., Torchia, M., Yang, S. L., DeArmond, S. J., and Prusiner, S. B. (1993) Propagation of prions with artificial properties in transgenic mice expressing chimeric PrP genes. *Cell* **73**, 979–988
43. Kocisko, D. A., Priola, S. A., Raymond, G. J., Chesebro, B., Lansbury, P. T., Jr., and Caughey, B. (1995) Species specificity in the cell-free conversion of prion protein to protease-resistant forms: a model for the scrapie species barrier. *Proc. Natl. Acad. Sci. U. S. A.* **92**, 3923–3927
44. Scott, M. R., Safar, J., Telling, G., Nguyen, O., Groth, D., Torchia, M., Koehler, R., Tremblay, P., Walther, D., Cohen, F. E., DeArmond, S. J., and Prusiner, S. B. (1997) Identification of a prion protein epitope modulating transmission of bovine spongiform encephalopathy prions to transgenic mice. *Proc. Natl. Acad. Sci. U. S. A.* **94**, 14279–14284
45. Vorberg, I., Groschup, M. H., Pfaff, E., and Priola, S. A. (2003) Multiple amino acid residues within the rabbit prion protein inhibit formation of its abnormal isoform. *J. Virol.* **77**, 2003–2009
46. Bruce, K. L., and Chernoff, Y. O. (2011) Sequence specificity and fidelity of prion transmission in yeast. *Semin. Cell Dev. Biol.* **22**, 444–451
47. Chang, H. Y., Lin, J. Y., Lee, H. C., Wang, H. L., and King, C. Y. (2008) Strain-specific sequences required for yeast [PSI⁺] prion propagation. *Proc. Natl. Acad. Sci. U. S. A.* **105**, 13345–13350
48. Tessier, P. M., and Lindquist, S. (2007) Prion recognition elements govern nucleation, strain specificity and species barriers. *Nature* **447**, 556–561
49. Chien, P., DePace, A. H., Collins, S. R., and Weissman, J. S. (2003) Generation of prion transmission barriers by mutational control of amyloid conformations. *Nature* **424**, 948–951
50. Verges, K. J., Smith, M. H., Toyama, B. H., and Weissman, J. S. (2011) Strain conformation, primary structure and the propagation of the yeast prion [PSI⁺]. *Nat. Struct. Mol. Biol.* **18**, 493–499
51. Prusiner, S. B., Scott, M., Foster, D., Pan, K. M., Groth, D., Mirenda, C., Torchia, M., Yang, S. L., Serban, D., Carlson, G. A., Hoppe, P. C., Westaway, D., and DeArmond, S. J. (1990) Transgenic studies implicate interactions between homologous PrP isoforms in scrapie prion replication. *Cell* **63**, 673–686
52. Collinge, J., and Clarke, A. R. (2007) A general model of prion strains and their pathogenicity. *Science* **318**, 930–936
53. Bett, C., Joshi-Barr, S., Lucero, M., Trejo, M., Liberski, P., Kelly, J. W., Masliah, E., and Sigurdson, C. J. (2012) Biochemical properties of highly neuroinvasive prion strains. *PLoS Pathog.* **8**, e1002522

Received for publication November 23, 2011.

Accepted for publication March 19, 2012.

Structure of the β 2- α 2 loop and interspecies prion transmission

Cyrus Bett, Natalia Fernández-Borges, Timothy D. Kurt, et al.

FASEB J 2012 26: 2868-2876 originally published online April 9, 2012

Access the most recent version at doi:[10.1096/fj.11-200923](https://doi.org/10.1096/fj.11-200923)

-
- Supplemental Material** <http://www.fasebj.org/content/suppl/2012/04/18/fj.11-200923.DC1>
- References** This article cites 52 articles, 20 of which can be accessed free at:
<http://www.fasebj.org/content/26/7/2868.full.html#ref-list-1>
- Subscriptions** Information about subscribing to *The FASEB Journal* is online at
<http://www.faseb.org/The-FASEB-Journal/Librarian-s-Resources.aspx>
- Permissions** Submit copyright permission requests at:
<http://www.fasebj.org/site/misc/copyright.xhtml>
- Email Alerts** Receive free email alerts when new an article cites this article - sign up at
<http://www.fasebj.org/cgi/alerts>
-



More than Lipids
Solutions for the entire product cycle:
Research to Commercialization



